Spectroscopic Studies of Actin–Metal–Nucleotide Complexes†

Joseph Loscalzo and George H. Reed*

ABSTRACT: Structural features of metal ion and nucleotide complexes with actin were investigated using electron paramagnetic resonance, water proton relaxation, and fluorescence techniques. Electron paramagnetic resonance spectra at 9.1 GHz (X band) of Mn(II) bound to the high affinity divalent cation site of F-actin were obtained from pellets of F-actin streaked along quartz supports. The line shape of these spectra showed a dependence on sample orientation in the magnetic field, indicating that some crystalline character is introduced into the sample with pellet streaking. A ^{55}Mn hyperfine coupling constant of 92 G was measured from spectra taken at 35.0 GHz (K band) and suggests that the coordination geometry for Mn(II) in F-actin is octahedral. An analysis of the temperature and frequency dependence of water proton relaxation rates in solutions of Mn(II)–F-actin revealed that above ~30 °C there is one water ligand in rapid exchange with bulk solvent. The paramagnetic contribution to the water proton relaxation rate exhibits an apparent activation energy of 5.2 kcal mol^{-1}, and this temperature dependence appears to reflect a structural equilibrium which either permits existing water ligands to exchange more readily above 30 °C or involves incorporation of an additional water ligand above 30 °C. The paramagnetic quenching effect of Mn(II) on the fluorescent ATP analogue, 1,N^6-ethenoadenosine triphosphate (ε-ATP), was used to determine the proximity of the nucleotide binding site to the high affinity divalent cation binding site on actin. Both in the Mn(II)–ε-ATP complex and the Mn(II)–ε-ATP–actin complex, the fluorescence intensity of ε-ATP was quenched by 32% compared with diamagnetic controls. Polymerization of actin did not affect the extent of quenching. These results suggest that the nucleotide and divalent cation bind to actin as a metal–nucleotide complex.

The interaction of divalent cations with actin has been the subject of extensive investigation during the past decade. Several key points have evolved from metal ion binding studies leading to the following general picture of the nature of actin–divalent cation interaction. Each actin monomer of molecular weight 42 000 (Elzinga et al., 1973) contains from five to seven low affinity ($K_D \sim 10^{-3}$ M) binding sites and one high affinity ($K_D \sim 10^{-5}$ M) site for divalent cations (Martonosi et al., 1964). Binding of divalent cations to the weaker affinity sites promotes polymerization of actin monomers (Oosawa and Kasai, 1971). On the other hand, the presence of a divalent cation at the high affinity site is essential for the structural integrity of the actin monomer (Kasai et al., 1965; Strzelecka-Golaszewska et al., 1974). In vivo, Mg(II) occupies the high affinity site (Weber et al., 1969), although other divalent cations can be readily substituted with the apparent order of affinity: Mn(II) ≥ Ca(II) > Cd(II) > Mg(II) > Zn(II) > Co(II) > Ni(II) (Kasai and Oosawa, 1968; Strzelecka-Golaszewska, 1973a). The presence of a divalent cation at the high affinity site also increases the affinity of actin for nucleotide (Asakura, 1961; Oosawa and Kasai, 1971) and influences the rate of nucleotide exchange (Strzelecka-Golaszewska, 1973b). With polymerization divalent cation bound at the high affinity site and bound nucleotide became virtually unexchangeable. Bound ATP is also hydrolyzed to ADP during the conversion of G-actin[1] to F-actin, although this hydrolysis is not an absolute requirement for the formation of F-actin (Kasai et al., 1965; Cooke, 1975). In contrast to the substantial amount of thermodynamic and kinetic data on metal ion–actin complexes (Oosawa and Kasai, 1971), there is much less information available on the structural aspects of these complexes. In the present paper structural features of metal ion and nucleotide complexes with actin are examined using the EPR and water proton relaxation rate enhancement characteristics of the Mn(II)–actin complex and the fluorescent properties of 1,N^6-ethenoadenosine nucleotides.

Materials and Methods

Protein Preparations. Actin was extracted as Ca(II)/Mg(II)-G-actin (40% Ca(II), 60% Mg(II) by atomic absorption spectroscopic analysis) from an acetone powder of rabbit skeletal muscle (Straub, 1942) at 4 °C with 10 mM Tris buffer, pH 8.5, 0.2 mM $CaCl_2$, 0.5 mM ATP, and 0.2 mM dithiothreitol. The extracted G-actin was polymerized with 0.1 M KCl and 2.0 mM $MgCl_2$, purified from the tropomyosin-troponin complex by centrifugation at 105 000*g* in the presence of 0.8 M KCl (Spudich and Watt, 1971), and depolymerized by a 3-day dialysis against the extraction solution.

Ca(II)/Mg(II)-G-actin was converted to Mg(II)-G-actin or Mn(II)-G-actin by diluting the G-actin approximately fivefold to 25 μM with 10 mM Tris buffer, pH 8.5, and 0.2 mM dithiothreitol, treating the solution with wet, anion-exchange resin in the chloride form (~25% of the actin solution's volume) followed by wet, cation-exchange resin in the sodium form (~10% of the actin solution's volume), and then incubating the

† From the Department of Biochemistry and Biophysics, University of Pennsylvania School of Medicine, Philadelphia, Pennsylvania 19174. *Received June 3, 1976.* This work was supported by grants from the United States Public Health Service, National Institutes of Health (HL 15835, AM 17517), by a Research Career Development Award to G.H.R. from the National Institutes of Health (1-KO4-AM70134), and by an M.S.T.P. award to J.L. from the National Institutes of Health (GM 02046-05-S1).

[1] Abbreviations used are: EPR, electron paramagnetic resonance; Tris, tris(hydroxymethyl)aminomethane; PRR, proton relaxation rate; NMR, nuclear magnetic resonance; G-actin, monomeric actin; F-actin, polymeric actin; Ca(II)/Mg(II)-actin, actin containing Ca(II) or Mg(II) at each high affinity divalent cation binding site; Mg(II)-actin, actin containing Mg(II) at each high affinity divalent cation binding site; Mn(II)-actin, actin containing Mn(II) at each high affinity divalent cation site; ε-ATP, 1,N^6-ethenoadenosine triphosphate; ε-ADP, 1,N^6-ethenoadenosine diphosphate; zfs, zero-field splitting; regulated actin, F-actin complexed with tropomyosin and troponin; subfragment 1, heavy meromyosin subfragment 1.

actin (~15 μM) with 75 μM $MgCl_2$ or 75 μM $MnCl_2$, respectively. A second cation-exchange resin treatment after polymerization with 0.1 M KCl removed virtually all excess Mg(II) or Mn(II) as well as displaced Mg(II) and Ca(II). The resulting Mg(II)-F-actin or Mn(II)-F-actin was sedimented as described above. The Mg(II)-F-actin and Mn(II)-F-actin typically contained 90–95% Mg(II) and Mn(II), respectively, as determined by atomic absorption spectroscopy of the supernatant of actin solutions in which the protein was precipitated with 0.5 N perchloric acid or liquid-scintillation analysis of ^{54}Mn added as $^{54}MnCl_2$ in the incubation step (~3.5 μCi/ml).

ϵ-ATP-G-actin was prepared by treating Ca(II)/Mg(II)-G-actin in 10 mM Tris buffer, pH 8.5, 0.2 mM $CaCl_2$, 0.2 mM ATP, and 0.2 mM dithiothreitol with wet, anion-exchange resin in the chloride form (~25% of the actin solution's volume) and then incubating the actin (~25 μM) with a fourfold molar excess (~100 μM) of ϵ-ATP. The actin was then converted to the Mg(II) or Mn(II) form by the procedure described above. Approximately 0.95 ϵ-ATP per actin molecule was found to be incorporated by fluorescence analysis of the supernatants of actin solutions adjusted to pH 8.0 in which protein was precipitated with 0.5 N perchloric acid.

Copolymers of different actin species were made by rapidly mixing the two populations of actin in the monomeric state and subsequently polymerizing with 0.1 M KCl after the addition of a small amount of F-actin (~5% of the total actin).

The tropomyosin-troponin complex was prepared according to the method of Ebashi and Ebashi (1964). Subfragment 1 was prepared as previously described (Loscalzo et al., 1975). Pellets of regulated actin were made by centrifuging F-actin mixed with a twofold weight excess of tropomyosin-troponin complex at 105 000g. Subfragment 1-F-actin pellets were made by centrifuging solutions of equimolar F-actin and subfragment 1 at 105 000g.

Magnetic Resonance Methods. X-band (9.1 GHz) and K-band (35.0 GHz) EPR spectra were recorded with Varian E-3 and 4503 spectrometers, respectively. Samples of actin suitable for EPR measurements were obtained by streaking a pellet of actin linearly on the flat surface of a Scanco S-807 quartz cell or, alternatively, by streaking the pellet along the inner wall of standard 3 mm i.d. or 2 mm i.d. quartz tubing.

The longitudinal relaxation times, T_1's, of water protons were recorded at 8.13, 15.0, 24.3, 40.0, and 60.0 MHz using a pulsed NMR spectrometer as described previously (Reuben and Cohn, 1970).

Fluorescence Measurements. Fluorescence spectra were recorded with a Perkin-Elmer MPF-2A ratio-recording spectrofluorimeter. Fluorescence intensity was taken as the height of the emission spectrum, in arbitrary units, at the wavelength of maximal emission. The excitation and emission bandwidths were 5 nm in all cases. The temperature of the sample was controlled by water which was temperature regulated and circulated with a Lauda-Brinkmann K-2/R circulator. All measurements were taken at 24 ± 1 °C. During temperature equilibration, the slits were closed and the sample was kept in darkness. The absorbance of the solutions never exceeded 0.12 using 0.4 cm path length cuvettes; hence, no correction for self-absorption of incident and emitted light was applied to the observed emission intensities.

Scatchard Analysis and Competition. Titrations of G-actin with Mn(II) or ϵ-ATP were performed in the presence of bound metal and nucleotide. The binding data for these titrations reflect a competition between added ligand and ligand already present in solution. The Scatchard equation (Scatchard, 1949) for ligand binding to a protein binding site(s) has the form:

$$\bar{\nu}_a/[A]_f = (n_a - \bar{\nu}_a)/K_a \quad (1)$$

where $\bar{\nu}_a = [A]_b/[P]_t$, [A] is the concentration of ligand, [P] is the protein concentration, the subscripts f, b and t, represent free, bound and total, respectively, n_a is the number of binding sites for A on P, and K_a is the dissociation constant for A binding to P. In the presence of competing ligand, B, which binds to the same site(s) as A, eq 1 can be rewritten as (cf. Reuben and Gabbay, 1975; Simonson et al., 1975):

$$\bar{\nu}_a/[A]_f = \frac{n_a}{K_a}\left(\frac{1}{1 + [B]_f/[K]_b}\right) - \frac{\bar{\nu}_a}{K_a}\left(\frac{1}{1 + [B]_f/[K]_b}\right) \quad (2)$$

where K_b is the dissociation constant for B binding to P.

In the absence of a competing ligand, the binding of A to P can be analyzed according to eq 1. A plot of $\bar{\nu}_a/[A]_f$ vs. $\bar{\nu}_a$ will be linear with a negative slope equal to K_a^{-1} and have an x intercept of n_a. Systems in which two different ligands with different affinities for the same site(s) compete are analyzed according to eq 2. This equation predicts that curvature should be evident in Scatchard plots of systems in which $[B]_f$ changes appreciably with respect to K_b over the range of $[A]_b$ examined. Systems in which $[B]_f$ changes insignificantly with respect to K_b will produce Scatchard plots with apparent K_a's which are different from the true K_a (i.e., that in the absence of inhibitor) and with n_a's which are not different from that in the absence of inhibitor. In the protein binding experiments described in this paper, conditions were chosen in order that the Scatchard plots produced have limited curvature.

Binding Measurements. Solutions of Ca(II)/Mg(II)-G-actin at 60 μM were titrated with $MnCl_2$. Since the amplitudes of EPR signals for Mn(II) bound to G-actin are much lower than those for $Mn(H_2O)_6^{2+}$, the residual signals for $Mn(H_2O)_6^{2+}$ in solutions of Mn(II) and G-actin can be used to determine the concentration of free $Mn(H_2O)_6^{2+}$ (Cohn and Townsend, 1954).

The affinity of G-actin for ϵ-ATP was determined by fluorescence techniques. Ca(II)/Mg(II)-G-actin (30 μM) was titrated with ϵ-ATP. Each sample was polymerized with 0.1 M KCl and subsequently treated with anion-exchange resin to remove unbound ϵ-ATP and displaced ATP. The supernatants of 0.5 N perchloric acid precipitates readjusted to pH 8.0 were analyzed by measuring the fluorescence intensity at 410 nm on excitation at 315 nm. A comparison of the measured intensities with those of free ϵ-ADP standards similarly treated with perchloric acid permitted a determination of the concentration of bound ϵ-ATP.

The affinity of ϵ-ATP for Mn(II) was determined by EPR techniques (Cohn and Townsend, 1954; Jallon and Cohn, 1970). The quenching of the fluorescence emission of ϵ-ATP by Mn(II) was also used as a measure of nucleotide-metal complex formation.

Analytical Methods. Protein concentrations were determined according to the method of Lowry (1951).

Viscosity measurements were performed in a water bath at 24 ± 1 °C with an Ostwald viscometer having a 60-s outflow time for water and a total volume of 10 ml.

Atomic absorption measurements were made with a Perkin-Elmer Model 403 atomic absorption spectrometer.

Radioactivity was measured in a Packard Tricarb Model 3385 liquid scintillation counter using Hydromix scintillation fluid (Yorktown Research, Hackensack, N.J.).

^{54}Mn was obtained from New England Nuclear (Boston,

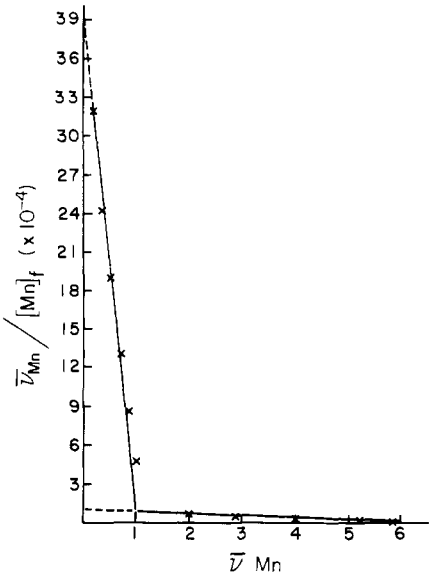

FIGURE 1: Scatchard plot of Mn(II) binding to G-actin in 10 mM Tris buffer, pH 8.0, and 0. 2 mM dithiothreitol at 23 °C. The G-actin concentration was 60 μM. Mn(II) binding was measured by the EPR technique described in Materials and Methods.

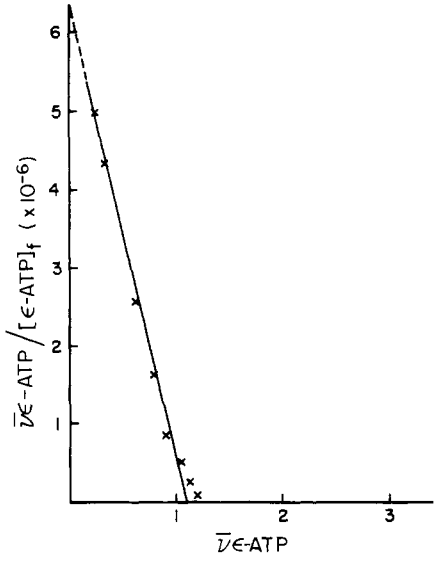

FIGURE 2: Scatchard plot of ϵ-ATP binding to G-actin in 10 mM Tris buffer, pH 8.0, and 0.2 mM dithiothreitol at 23 °C. The G-actin concentration was 30 μM. ϵ-ATP binding was measured by the fluorescence technique described in Materials and Methods.

Mass.) and ϵ-ATP and ϵ-ADP were from Sigma Chemical Co. (St. Louis, Mo.). The purity of ϵ-ATP and ϵ-ADP was checked by polyethyleniminecellulose thin-layer chromatography as described by Randerath and Randerath (1967).

Results

Binding Measurements. Substitution[2] of Mn(II) into Ca(II)/Mg(II)-G-actin was monitored by the decrease in amplitude of the EPR signal for free $Mn(H_2O)_6^{2+}$ (see Materials and Methods). The data are shown in the form of a Scatchard plot in Figure 1. Two classes of binding sites are indicated with stoichiometries of one and approximately five and apparent dissociation constants of 2.6 μM and 0.6 mM, respectively, although the extent to which free Ca(II) and Mg(II) changes with respect to its dissociation constant for G-actin may influence the apparent dissociation constant for the weaker sites substantially.

Substitution[2] of ϵ-ATP into G-actin was analyzed by fluorescence (see Materials and Methods). A Scatchard plot of the data is shown in Figure 2 and indicates a single binding site with an apparent dissociation constant of 0.16 μM.

Data for the binding of Mn(II) to ϵ-ATP obtained by EPR and fluorescence measurements are shown in Figure 3. The coincidence of these data demonstrates a one-to-one relationship between the quenching of ϵ-ATP fluorescence by Mn(II) and the formation of a Mn(II)-ϵ-ATP complex.

EPR Spectra of the Mn(II)-F-Actin Complex. The EPR signals for Mn(II) bound to actin are not isotropically averaged (cf. Reed and Cohn, 1970; Reed and Ray, 1971). EPR signals for this complex are, therefore, difficult to obtain in solution since solutions of G-actin of sufficient concentration to permit observation of bound Mn(II) polymerize and solutions of F-actin of sufficient concentration for EPR observation of the bound Mn(II) are extremely viscous. However, the spectrum (Figure 4) is readily obtained from a pellet of F-actin which

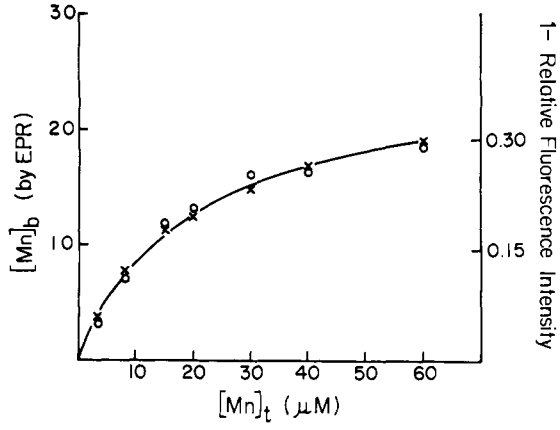

FIGURE 3: Binding isotherm for the interaction of Mn(II) and ϵ-ATP in 10 mM Tris buffer, pH 8.0, and 0.2 mM dithiothreitol at 23 °C. The ϵ-ATP concentration was 20 μM. Mn(II)-ϵ-ATP complex formation was measured both by the decrease in the EPR signal of $Mn(H_2O)_6^{2+}$ (X) and the decrease in the fluorescence intensity of ϵ-ATP (O) (excitation 315 nm; emission 210 nm).

is streaked along the surface of a quartz support. The spectrum for the protein-bound Mn(II) is easily differentiated from that for free $Mn(H_2O)_6^{2+}$ in a similar pellet (Figure 4C).

Powder type EPR line shapes are expected for Mn(II)-protein complexes for which there is a random orientation of the molecular axis of the complex in the magnetic field (Reed and Cohn, 1970). Since a powder line shape already represents the solid angle-weighted sum over all possible orientations of the molecular axis in the external magnetic field (Taylor et al., 1975), the EPR spectrum for a powder sample does not change with orientation. However, the line shape of the EPR spectrum for Mn(II)-F-actin in streaked[3] pellets does change with sample orientation (Figure 4, inset). The shear forces involved in streaking the pellet are apparently sufficient to effect alignment of the actin filaments (Burley et al., 1971). Although the exact orientation of the filaments within the sample is not

[2] Since G-actin free of metal or nucleotide rapidly denatures, binding studies of metal or nucleotide to G-actin could not be performed with metal or nucleotide-free G-actin; hence, all dissociation constants are apparent (see Materials and Methods for further discussion).

[3] If the Mn(II)-F-actin pellet is not streaked but simply applied to the quartz support, no orientation dependence is observed.

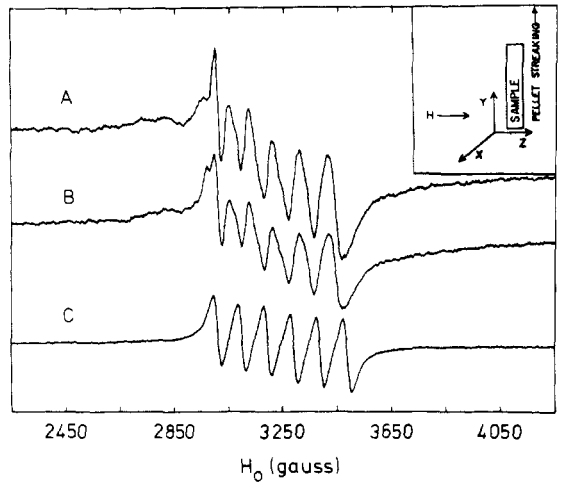

FIGURE 4: X-band EPR spectra of Mn(II)-F-actin and of $Mn(H_2O)_6^{2+}$ in a pellet of Ca(II)/Mg(II)-F-actin. (A) Streaked pellet of Mn(II)-F-actin (~1 mM); (B) same sample as A with a 90° rotation about the y axis (see Figure 5); (C) $Mn(H_2O)_6^{2+}$ (~1.2 mM) in a pellet of Ca(II)/Mg(II)-F-actin. The sample temperature was 16 °C in all cases. The inset schematically represents the geometry of streaking of pellets and of sample placement in the magnetic field, H.

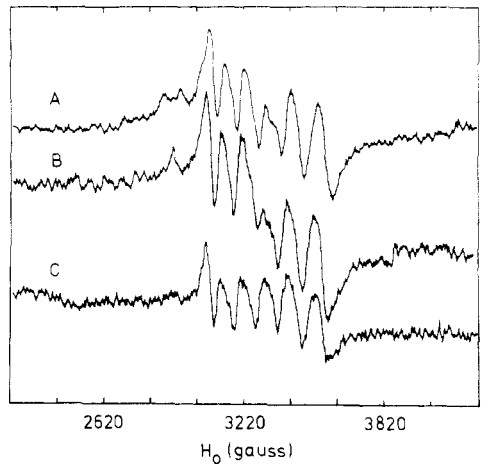

FIGURE 5: X-band EPR spectra for a streaked pellet of Mn(II)-regulated actin at three different sample orientations in the magnetic field, 0, 90, and 120° relative orientations for A, B, and C, respectively. Sample temperature was 20 °C in all cases. Note the changes in the positions of the peaks to the low-field side of the central transition and the changes in relative amplitudes and shapes of the central hyperfine transitions.

known, it is likely that the filaments are aligned approximately parallel to the direction of streaking. The geometry of the sample with respect to the magnetic field is sketched in the inset of Figure 4. Rotations about the y axis produce the changes in the EPR spectrum of Mn(II) which are apparent in the spectra of Figure 4A and 4B. It is surprising to find an orientation dependence about the y axis since this implies that there is sample order in the plane perpendicular to y. Furthermore, the helical arrangement of monomers in the filament would already sample several angles in the x-z plane. However, an inexact alignment of the filaments along y could also account for these observations.

The six hyperfine components of the $M_s = -\frac{1}{2} \leftrightarrow M_s = +\frac{1}{2}$ fine structure transition (where M_s is the electron spin quantum number) constitute the dominant transitions in the spectra for pellets of Mn(II)-F-actin. There are, however, weaker signals to the low-field side of the central ($-\frac{1}{2} \leftrightarrow +\frac{1}{2}$) set which are assigned[4] to the $M_s = +\frac{3}{2} \leftrightarrow M_s = +\frac{1}{2}$ fine structure transition. The positions of these latter signals exhibit a strong dependence on sample orientation because of their first-order dependence on the zfs anisotropy (cf. Howling, 1969). In contrast, the central fine structure transition shows a less pronounced orientation dependence since the anisotropy for this transition arises solely from second-order terms in the zfs.[5]

Streaked pellets of regulated actin give orientation dependent spectra (Figure 5) similar to those for F-actin. In fact, in our experience the fidelity of alignment of filaments is typically greater for regulated actin than for F-actin.

The concentration of Mn(II) in pellets of the subfragment 1-Mn(II)-F-actin complex is at least fourfold more dilute than in Mn(II)-F-actin. Thus far, the signal for the subfragment 1-Mn(II)-F-actin samples have been too weak for any quantitative statements about the influence of subfragment-1 binding on the spectrum of Mn(II) bound to F-actin.

There is improved resolution of the $\frac{1}{2} \leftrightarrow -\frac{1}{2}$ fine structure transition in the K-band EPR spectrum (not shown) for a streaked pellet of Mn(II)-F-actin. The improved resolution in the K-band spectrum is expected because second-order terms in the zfs are reduced by a factor of approximately four at K band relative to their contributions at X band. A ^{55}Mn hyperfine coupling constant of 92 G is measured from the sextet splitting of the $\frac{1}{2} \leftrightarrow -\frac{1}{2}$ transition in the K-band spectrum.

Frequency and Temperature Dependence of Water PRR. Mn(II) bound to F-actin influences the longitudinal PRR of water. In order to determine whether or not this relaxation effect originates from an exchange of water molecules between the first coordination sphere of bound Mn(II) and the bulk solvent, the temperature and frequency dependencies of the water PRR were examined (Reuben and Cohn, 1970). The relationship between the paramagnetic contribution to the PRR, $1/T_{1p}$, and the relaxation rate of water protons in the first coordination sphere of Mn(II), $1/T_{1M}$, is given by the Swift-Connick equation:

$$1/T_{1p} = nP_M/(T_{1M} + \tau_m) \quad (3)$$

where n is the number of water molecules in the first coordination sphere, nP_M is the mole fraction of water molecules bound to the ion, and τ_m is the residence time for a water molecule in the first coordination sphere of the ion (Swift and Connick, 1962).

When $T_{1M} \gg \tau_m$ (i.e., fast exchange conditions prevail), then from the Solomon-Bloembergen equation (Solomon, 1955; Bloembergen, 1957):

$$1/T_{1P} = 1/3B\tau_c(1 + \omega_I^2\tau_c^2) \quad (4)$$

over a frequency range from 8 to 60 MHz (Peacocke et al., 1969). In eq 4, B contains constants[6] characteristic of the

[4] The sign of D, the axial distortion parameter for the zfs, is arbitrarily chosen as negative.

[5] The general form of the second-order terms in the zfs for $M_s = \frac{1}{2} \rightarrow M_s = -\frac{1}{2}$ transition is: $(4.00/H_0)[(D - E\cos 2\phi)^2 \sin^2 2\theta + 4E^2 \sin^2\theta \sin^2 2\phi] - (2.00/H_0)\{[D\sin^2\theta + E\cos 2\phi(1 + \cos^2\theta)]^2 + 4E^2\cos^2\theta\sin^2 2\phi\}$, where H_0 is the unperturbed resonance position given by $h\nu/g\beta$, D, E represent the axial and rhombic distortions, respectively, in the symmetry of the ligand field, and θ and ϕ are the polar and azimuthal angles, respectively. The orientation dependence of the central fine structure transition in the regulated actin sample is manifested in changes in the relative amplitudes and shapes of the six hyperfine components.

[6] For water protons at a distance of 2.48 Å from the center of Mn(II), B has a value of 9.48×10^{12} M^{-1} s^{-2} per water molecule.

TABLE I: Relative Fluorescence Intensity of ϵ-ATP and ϵ-ADP Complexed with Mg(II), Mn(II), and Actin.

Complex[a]	Rel Fluor Inten
Mg(II)-ϵ-ATP	1.00
Mn(II)-ϵ-ATP	0.68
Mg(II)-ϵ-ADP	1.00
Mn(II)-ϵ-ADP	0.68
ϵ-ATP-Mg(II)-G-actin	0.99
ϵ-ATP-Mn(II)-G-actin	0.67
ϵ-ADP-Mg(II)-F-actin	0.70
ϵ-ADP-Mn(II)-F-actin	0.38

[a] The fluorescence of free metal-nucleotide complexes was measured in solutions of 80 μM ϵ-ATP and 10 mM $MgCl_2$ or 1 mM $MnCl_2$ at a total ionic strength of 0.14. The fluorescence of the protein-bound metal-nucleotide complexes was measured in a solution of 10 μM G-actin containing essentially stoichiometric bound metal and nucleotide immediately (within 5 s) after ion-exchange resin treatment and subsequent dilution from a 20 μM stock solution. Since the off-rates for metal and nucleotide from G-actin are relatively slow (Loscalzo et al., 1975; Bárány et al., 1962) with half-times of ~0.5 min, the rapidity with which these measurements were performed limited the contribution by free fluorescent nucleotide to the total fluorescence intensity to no more than a few percent. Solutions of F-actin at 10 μM were also used in these experiments but, since the bound metal and nucleotide are effectively unexchangeable when bound to the actin polymer (except for a small contribution from the free monomer in equilibrium with polymer (~1 μM)), similar precautions as observed with solutions of G-actin were not necessary.

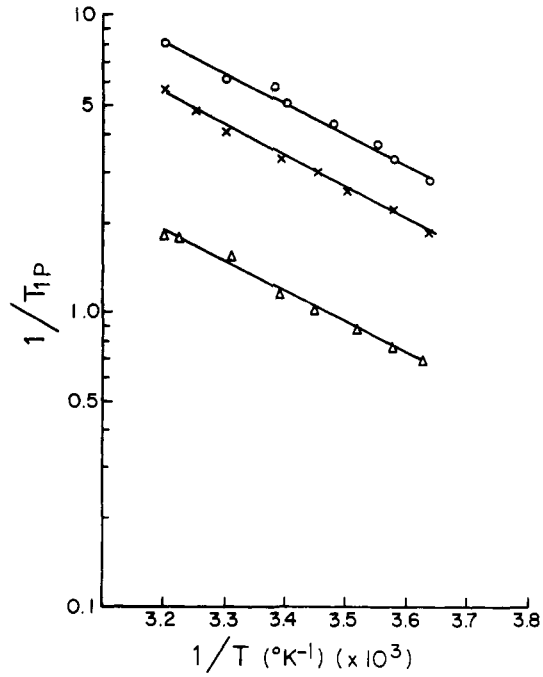

FIGURE 6: Temperature dependence of the logarithm of the paramagnetic contribution to the proton relaxation rate for water, $1/T_{1P}$, for Mn(II)-F-actin at three different frequencies, 8.14 MHz (○), 24.3 MHz (X), and 60.0 MHz (△). The solution contained 50 μM Mn(II)-F-actin (with 0.95 mol of Mn(II) per mol of actin), 10 mM Tris buffer, pH 8.0, 0.1 M KCl, and 0.2 mM dithiothreitol.

electron and nuclear spins, the inverse sixth power of the distance between the water protons and Mn(II), and the mole fraction of water molecules bound to the ion, ω_I is the nuclear Larmor frequency, and τ_c is the correlation time[7] for modulation of the electron-nuclear dipolar coupling. For a frequency-independent correlation time, eq 4 predicts a linear relationship between T_{1P} and ω_I^2, and the ratio of the slope to intercept of a plot of T_{1P} vs. ω_I^2 gives τ_c^2 (Peacocke et al., 1969). Since T_{1M} is an explicit function of ω_I and τ_m is independent of frequency, a frequency dependence of $1/T_{1P}$ eliminates the possibility that $1/T_{1P}$ is completely exchange limited; i.e., τ_m cannot be much greater than T_{1M} (see eq 3). Figure 6 shows Arrhenius plots, $1/T_{1P}$ vs. $1/T$, for three different frequencies. The data show that $1/T_{1P}$ is frequency dependent. The apparent activation energies from the slopes of the plots, ~5.2 kcal mol^{-1}, are of the proper magnitude to suggest a possible involvement of a τ_m process (Zetter et al., 1972). However, the fact that the three Arrhenius plots of Figure 6 are approximately parallel shows that fast exchange conditions are satisfied.[8] Values of τ_c evaluated from the square root of the ratio of the slope to intercept of the data of Figure 6 plotted as T_{1P} vs. ω_I^2 range from 4.4×10^{-9} s at 3 °C to 5.1×10^{-9} s at 40 °C which correspond to a much lower activation energy for τ_c than that observed for $1/T_{1P}$ itself. Hence the slopes of the plots in Figure 6 do not correspond to the activation energy for τ_c or for a τ_m limited exchange process. The assumption which is implicit in the variable-temperature study is that the tertiary structure of the complex remains constant over the range of temperature of the measurements. Values of the hydration number, n, obtained from the magnitude of the relaxation rate and the correlation times (see eq 4), vary from 0.4 to 1.4 between 3 and 40 °C. This increase in the value of n with temperature together with the anomalous temperature profile of $1/T_{1P}$ suggests that the structure of the binding site for Mn(II) in F-actin changes with temperature.

Fluorescence Studies. ϵ-ATP readily substitutes for ATP in G-actin without loss of actin polymerizability (Thames et al., 1974) and with a dissociation constant not very different from that for ATP (Oosawa and Kasai, 1971). When bound to G-actin, the fluorescence intensity at 410 nm (excitation at 315 nm) does not change. Actin polymerization, accompanied by the conversion of ϵ-ATP to ϵ-ADP, leads to a 30% decrease in the fluorescence intensity of the bound ϵ-ADP relative to free ϵ-ADP (and ϵ-ATP) (Thames et al., 1974).

When complexed with Mn(II), a 32% reduction in fluorescence intensity of ϵ-ATP (and ϵ-ADP) occurs. In order to ascertain the proximity of the high affinity divalent cation binding site to the nucleotide binding site of actin, the fluorescence intensity of ϵ-ATP (ϵ-ADP) was examined when bound to Mg(II) and Mn(II)-F-actin. Table I shows the results of these experiments: Mn(II) quenches the fluorescence of ϵ-ATP (ϵ-ADP) at 410 nm (excitation at 315 nm) to the same extent in the metal-nucleotide complex as in the metal-nucleotide-actin complex. That bound Mn(II) quenches the fluorescence of bound nucleotide to the same relative extent in both G and F-actin suggests that Mn(II) on one monomer is not interacting with the nucleotide of an adjacent monomer. Copolymer experiments were performed to confirm the intrasubunit nature of the fluorescence quenching. With copolymers of F-actin in which ϵ-ADP-Mg(II)-containing monomers were diluted tenfold with monomers containing Mn(II) and nonfluorescent ADP, the fluorescence intensity of the bound ϵ-ADP (0.96 relative fluorescence intensity) was essentially unchanged from that of pure ϵ-ADP-Mg(II)-F-actin

[7] τ_c is defined as: $1/\tau_c = 1/\tau_m + 1/\tau_r + 1/\tau_s$, where τ_m is defined above, τ_r is the rotational correlation time for Mn(II) in the Mn(II)-protein complex, and τ_s is the electron spin lattice relaxation time.

[8] One expects maximal exchange limitation at lower frequencies since T_{1M} is smaller at lower frequencies than at higher frequencies (see eq 1).

normalized to one-tenth the total copolymer concentration (1.00 relative fluorescence intensity). Copolymers of ϵ-ADP-Mn(II)-containing monomers diluted tenfold with ADP-Mg(II)-containing monomers exhibited a reduction in ϵ-ADP fluorescence intensity (0.69 relative fluorescence intensity) essentially similar to that of pure ϵ-ADP-Mn-(II)-F-actin normalized to one-tenth the total copolymer concentration (0.72 relative fluorescence intensity). The slight differences between copolymers and pure F-actins reflect the mild exchange of divalent cations and nucleotides between unpolymerized monomers during polymerization (k_{off}(nucleotide-G-actin) = 0.015 s^{-1} (Bárány et al., 1962); k_{off}(Mn(II)-G-actin) = 0.029 s^{-1} (Loscalzo et al., 1975)). Equivalent time courses for polymerization among both types of copolymers and pure F-actins monitored by viscosimetry suggest that random copolymers formed during these experiments (Loscalzo et al., 1975).

Discussion

The Mn(II)-G-actin and ϵ-ATP-G-actin complexes exhibit apparent dissociation constants which are of the same order of magnitude as those for their physiological counterparts, Mg(II)-G-actin and ATP-G-actin, respectively. Furthermore, these two substitutions appear to be innocuous with respect to actin polymerizability (Thames et al., 1974) and cofactor activation of subfragment 1-Mg(II)-ATPase (J. Loscalzo, unpublished observation). Once actin is polymerized, the divalent metal ion and nucleotide moieties become virtually unexchangeable. This property facilitates spectroscopic studies since there is no interference from the free metal ion or nucleotide.

Because of the solid state character of the EPR line shape for Mn(II)-F-actin, concentrations of bound Mn(II) of the order of 0.5 to 1 mM are required for reasonable EPR signals. Such concentrations are most easily achieved in pellets of F-actin obtained by centrifugation at 105 000g. EPR spectra for pellets of F-actin streaked along a quartz support exhibit an orientation dependence which indicates that streaking introduces a considerable degree of order in the sample. The EPR line shape is a hybrid with features characteristic of single crystal and of powder samples. It is also noteworthy that streaked pellets of regulated actin routinely give spectra which indicate a higher degree of order than do spectra for unregulated actin filaments. The 92-G ^{55}Mn hyperfine coupling constant for Mn(II)-F-actin suggests that the coordination geometry for Mn(II) is octahedral (van Wieringen, 1955).

Water proton relaxation rate measurements for solutions of Mn(II)-F-actin give an indication of the ease of accessibility of solvent to the site of the nondissociable cation and of the hydration number of the bound cation. Above ~30 °C the apparent hydration number for Mn(II) obtained from the water PRR data is greater than unity, suggesting that there is one water ligand in rapid exchange with the bulk solvent. Although the paramagnetic contribution to the PRR has an apparent activation energy of ~5.2 kcal mol^{-1}, the origin of this temperature dependence appears to be a structural equilibrium which either permits existing water ligands to exchange in its high temperature state or involves addition of a water ligand in the high-temperature state. Since there are probably outer sphere contributions to the PRR at all temperatures, the quantitative significance of the fractional hydration numbers obtained below ~30 °C is not clear.

The virtual equivalence of the extent of quenching of ϵ-ATP fluorescence by Mn(II) in the free Mn(II)-nucleotide complex and in the ternary complex with actin indicates a close proximity of the divalent cation and nucleotide binding sites on actin. In fact, these data indicate that Mn(II) and ϵ-ATP bind to actin as a metal-nucleotide complex. While it is tempting to suggest that the free metal-nucleotide and actin-bound metal-nucleotide complexes have similar conformations, no suitable quantitative description of fluorescence quenching by paramagnetic ions is available to substantiate this interpretation (Bennick et al., 1971; Green et al., 1973).

Acknowledgments

The authors express their thanks to Drs. Annemarie Weber and Clive Bagshaw for stimulating discussions and helpful comments.

References

Asakura, S. (1961), *Arch. Biochem. Biophys. 92,* 140-149.
Bárány, M., Finkelman, F., and Therattil-Antony, T. (1962), *Arch. Biochem. Biophys. 98,* 28-45.
Bennick, A., Campbell, I. D., Dwek, R. A., Price, N. C., Radda, G. K., and Salmon, A. G. (1971), *Nature (London), New Biol. 234,* 140-143.
Bloembergen, N. (1957), *J. Chem. Phys. 27,* 572-573, 595-596.
Burley, R. W., Siedel, J. C., and Gergely, J. (1971), *Arch. Biochem. Biophys. 146,* 597-602.
Cohn, M., and Townsend, J. (1954), *Nature (London) 173,* 1090-1091.
Cooke, R. (1975), *Biochemistry 14,* 3250-3256.
Ebashi, S., and Ebashi, R. (1964), *J. Biochem. (Tokyo) 53,* 604-613.
Elzinga, M., Collins, J. H., Kuehl, W. M., and Adelstein, R. S. (1973), *Proc. Natl. Acad. Sci. U.S.A. 70,* 2687-2691.
Green, J. A., Singer, L. A., and Parks, J. H. (1973), *J. Chem. Phys. 58,* 2690-2695.
Howling, D. H. (1969), *J. Magn. Reson. 1,* 339-355.
Jallon, J. M., and Cohn, M. (1970), *Biochim. Biophys. Acta 222,* 542-545.
Kasai, M., Nakano, E., and Oosawa, F. (1965), *Biochim. Biophys. Acta 94,* 494-503.
Kasai, M., and Oosawa, F. (1968), *Biochim. Biophys. Acta 154,* 520-528.
Loscalzo, J., Reed, G. H., and Weber, A. (1975), *Proc. Natl. Acad. Sci. U.S.A. 72,* 3412-3415.
Lowry, O. H., Rosebrough, N. J., Farr, A. L., and Randall, R. J. (1951), *J. Biol. Chem. 193,* 265-275.
Martonosi, A., Molino, C. M., and Gergely, J. (1964), *J. Biol. Chem. 239,* 1057-1064.
Oosawa, G., and Kasai, M. (1971), in Subunits in Biological Systems, Timasheff, S. N., and Fassman, G. D., Ed., New York, N.Y., Marcel Dekker, pp 261-322.
Peacocke, A. R., Richards, R. E., and Sheard, B. (1969), *Mol. Phys. 16,* 177-189.
Randerath, K., and Randerath, E. (1967), *Methods Enzymol. 129,* 323-347.
Reed, G. H., and Cohn, M. (1970), *J. Biol. Chem. 245,* 662-664.
Reed, G. H., and Ray, W. J., Jr. (1971), *Biochemistry 10,* 3190-3197.
Reuben, J., and Cohn, M. (1970), *J. Biol. Chem. 245,* 6539-6546.
Reuben, J., and Gabbay, E. J. (1975), *Biochemistry 14,* 1230-1235.
Scatchard, G. (1949), *Ann. N.Y. Acad. Sci. 51,* 660-672.
Simonson, L. P., Bär, H., Jastorff, B., and Hitkari, R. (1975),

Biochim. Biophys. Acta 379, 114-124.
Solomon, I. (1955), *Phys. Rev. 99,* 559-565.
Spudich, J. A., and Watt, S. (1971), *J. Biol. Chem. 246,* 4866-4871.
Straub, F. B. (1942), *Stud. Inst. Med. Chem. Univ. Szeged. 2,* 3-22.
Strzelecka-Golaszewska, H. (1973a), *Biochim. Biophys. Acta 310,* 60-69.
Strzelecka-Golaszewska, H. (1973b), *Eur. J. Biochem. 37,* 434-440.
Strzelecka-Golaszewska, H., Nagy, B., and Gergely, J. (1974), *Arch. Biochem. Biophys. 161,* 559-569.
Swift, T. J., and Connick, R. E. (1962), *J. Chem. Phys. 37,* 307-320.
Taylor, P. C., Baugher, J. F., and Kriz, H. M. (1975), *Chem. Rev. 75,* 203-240.
Thames, K. E., Cheung, H. C., and Harvey, S. C. (1974), *Biochem. Biophys. Res. Commun. 60,* 1252-1261.
van Wieringen, J. S. (1955), *Discuss. Faraday Soc. 19,* 118-126.
Weber, A., Herz, R., and Reiss, I. (1969), *Biochemistry 8,* 2266-2271.
Zetter, M. S., Grant, M. W., Wood, E. J., Dodgen, H. W., and Hunt, J. P. (1972), *Inorg. Chem. 11,* 2701-2706.

Interactions between Pancreatic Lipase, Co-Lipase, and Taurodeoxycholate in the Absence of Triglyceride Substrate†

Jakob Donnér,*,§ Charles H. Spink,‡ Bengt Borgström,§ and Ingvar Sjöholm¶

ABSTRACT: We have studied the interactions between lipase, co-lipase, and taurodeoxycholate by calorimetry and circular dichroism determinations. Porcine pancreatic lipase binds to co-lipase to form a 1:1 complex with an association constant of 2×10^6 M^{-1}. The binding is exothermic and proceeds with an increase of entropy and the ΔC_p of the reaction is highly negative, -1.31 kJ K^{-1} (mol of lipase)$^{-1}$ at 25 °C. This is interpreted to be due to hydrophobic interactions between lipase and co-lipase. The binding of taurodeoxycholate to lipase and co-lipase is an endothermic process, which proceeds without any gross conformational changes as judged by circular dichroism measurements, although spectral changes are observed in the aromatic region. No binding between taurodeoxycholate and co-lipase is detected until concentrations near the critical micellar concentration of the former are reached. It is suggested that taurodeoxycholate and co-lipase form mixed micelles.

Pancreatic lipase (EC 3.1.1.3), which preferentially hydrolyzes water-insoluble esters of fatty acids in the diet, is inhibited by conjugated bile salts, which are normally found in the duodenal contents. The lipase activity is restored in the presence of a polypeptide cofactor, co-lipase. Co-lipase also enhances lipase activity in the absence of bile salts (Borgström and Erlanson, 1973). The system lipase-co-lipase-bile salt-substrate surface involves several important binding reactions, the nature of which are not well understood. Recently, equilibrium dialysis experiments were employed to elucidate the characteristics of the binding between some conjugated bile salts and lipase and co-lipase, respectively (Borgström and Donnér, 1975). As far as co-lipase-bile salt interactions are concerned, the results of these experiments have been confirmed by interaction studies in the ultracentrifuge (Charles et al., 1975).

In order to provide a basis for a better understanding of the effect of the different binding reactions mentioned above on the enzymatic activity, the lipase-co-lipase-bile salt system was studied by calorimetry and circular dichroism measurements.

Experimental Procedure

Porcine pancreatic lipase L_B was prepared by a modification (Donnér, 1976) of the method of Verger et al. (1969); the lipase obtained was free of co-lipase activity. Porcine pancreatic co-lipase was purified as described by Erlanson and Borgström (1972) and TDC[1] was synthesized by us (Norman, 1955). Sodium dodecyl sulfate of approximately 95% purity was recrystallized three times from 95% ethanol (Ray et al., 1966).

Protein concentration was determined spectrophotometrically using $E_{280nm}^{1\%} = 13.3$ for lipase and $E_{280nm}^{1\%} = 4.2$ for co-lipase. The molecular weights for lipase and co-lipase were taken to be 52 000 and 11 260, respectively. The solutions were stored at +4 °C. All experiments were carried out at pH 7.0.

In the calorimetric experiments, solutions of lipase, co-lipase, and TDC were made such that the final buffer composition was 2 mM Tris-HCl, 150 mM NaCl, 1 mM $CaCl_2$, and 0.02%

†From the Department of Physiological Chemistry and the Department of Thermochemistry, University of Lund, Lund, and the Department of Pharmaceutical Biochemistry, University of Uppsala, Uppsala, Sweden. *Received June 28, 1976.* This work was supported by Dr. Påhlssons Stiftelse and the Medical Faculty at the University of Lund.

‡Present address: Chemistry Department, State University of New York at Cortland, Cortland, New York.
§Department of Physiological Chemistry 4, P. O. Box 750, S-220 07 Lund 7, Sweden.
¶Department of Pharmaceutical Biochemistry, Box 578, S-751 23 Uppsala, Sweden.

[1]Abbreviations used: TDC, sodium taurodeoxycholate; cmc, critical micellar concentration; CD, circular dichroism; Tris-HCl, tris(hydroxymethyl)aminomethane hydrochloride; UV, ultraviolet; NMR, nuclear magnetic resonance.